Complete model of a self-gravitating cosmic string: A new class of exact solutions

Charles C. Dyer and Francine R. Marleau
Department of Astronomy, University of Toronto, 60 St. George Street, Toronto, Ontario, Canada M5S 1A7
(Received 4 November 1994; revised manuscript received 12 April 1995)

We find solutions of Einstein's field equation for topologically stable strings associated with the breaking of a U(1) symmetry. Strings form in many GUT's and are expected whenever the homotopy group $\Pi_1(M_0)$ is nontrivial. The behavior of the fields making up the string is described by the Euler-Lagrange equations. These fields appear in the energy-momentum tensor so we must solve simultaneously for the coupled Einstein-scalar-gauge field equations. Numerical results are obtained using a Taylor-series method. We obtain a five-parameter family of solutions and discuss the assumption of regularity at the origin. Finally, we introduce the idea of gravitational lensing near the center of the string as a possible physical effect.

PACS number(s): 11.27.+d, 95.30.Sf, 98.80.Cq

I. INTRODUCTION

Phase transitions occur in the early universe as a consequence of its expansion and cooling. The transitions cannot be observed directly but can be inferred from the theory of groups and symmetries in elementary particle physics. If these phase transitions do occur, topological defects will necessarily form during the transition. These defects take their name after their characteristic of being trapped regions of "old symmetry" surrounded by "new symmetry." In essence, they retain the characteristics of the state of the universe as it was before the phase transition. The topology of the defect varies according to the symmetry group G characterizing the fields present in the universe before the symmetry breaking and the symmetry group H which describes the symmetry of the field after the symmetry breaking; i.e., H includes all elements of G which leave the vacuum expectation value of the scalar field invariant. When the first homotopy group is nontrivial, $\Pi_1(G/H) \neq I$, i.e., the topological know cannot be "unwound," the topology of the defect is linear, or stringlike. Topologically stable strings occur in non-Abelian gauge theories such as SU(5) (Shafi and Vilenkin [1]) and SO(10) (Kibble, Lazarides, and Shafi [2]) grand unified theories but also in the simple case of Abelian U(1) symmetry.

The gravitational field of strings has been studied in general relativity starting with the work of Vilenkin [3], subsequent to the Newtonian approach to topological defects given by Zel'dovich *et al.* [4] and Kibble [5]. He used the linear approximation of general relativity and an energy-momentum tensor which has no lateral stresses but only terms describing the energy density and the pressure (tension) along the axis of the string. This assumption was used later in work such as that of Gott [6] and Hiscock [7] in looking for exact solutions of Einstein's equations for a string where, in addition, the energy density of the string was taken to be constant. It has since been shown by Raychaudhuri [8] that the Gott and Hiscock solution is not consistent with proper boundary conditions.

Subsequently, there have been a number of attempts to obtain better models of cosmic strings. These range from treatments which impose a fixed background geometry wherein the properties of the string are calculated, to the attempt of Laguna-Castillo and Matzner [9] and Garfinkle and Laguna [10] who alternately held the metric functions fixed while integrating the string equations and held the string field properties fixed while computing the new metric from the Einstein equations.

The purpose of this paper is to extend previous attempts at describing gravitating cosmic strings by simultaneously solving the coupled Einstein-scalar-gauge field equations, so that our model will include the effect of the energy-momentum of the string on the background. In addition, we want to study the physical properties of the string solutions that emerge from this set of differential equations. Recently, Shaver [11] has examined the equations for nonstationary cosmic strings and solved them for the simple energy-momentum tensor introduced by Vilenkin. Based on the general set of equations obtained by Shaver and dropping the Vilenkin restrictions to the form of the energy-momentum tensor, we will use a numerical integration technique to attempt to find all possible solutions for self-gravitating strings.

II. THE COUPLED EINSTEIN-SCALAR-GAUGE FIELD EQUATIONS

We will be studying string topological defects associated with the spontaneous symmetry breaking of an Abelian group $G = \mathrm{U}(1)$. The Lagrangian of this Abelian-Higgs model is

$$L = -\frac{1}{2}(D^\mu\Phi)^*(D_\mu\Phi) - V(\Phi) - \frac{1}{2}F_{\mu\nu}F^{\mu\nu} \ , \qquad (1)$$

where $F_{\mu\nu} = \nabla_\mu A_\nu - \nabla_\nu A_\mu$, $D_\mu = \nabla_\mu + ieA_\mu$, $V(\Phi)$ is the potential of the scalar field, A_μ is the gauge field, e the gauge coupling constant, and Φ the scalar field. The symmetry breaking potential has the form $V(\Phi) =$

$\lambda(\Phi^*\Phi-\eta^2)^2$ where λ is the self-coupling constant of the Higgs field and η is the value of the symmetry-breaking Higgs field. Shaver [11] has shown that for the specific choice of the energy-momentum tensor given by Vilenkin [3], $\lambda=e^2/8$. Since we are concerned with finding solutions where T^r_r and T^ϕ_ϕ are not necessarily zero, we will set $\lambda=\alpha e^2/8$ where α is a constant and can be taken as a free parameter. Note that, when acting on a scalar field, ∇_μ simply becomes ∂_μ. Also, because of the symmetries of the Christoffel symbols, $\nabla_\mu A_\nu-\nabla_\nu A_\mu=\partial_\mu A_\nu-\partial_\nu A_\mu$.

The spontaneous symmetry breaking is obtained by introducing the Higgs field. The symmetry of the system after such a breaking is then determined by the degeneracy of the vacuum expectation value of the scalar field:

$$\Phi=|\Phi|e^{i\theta},\quad 0\le\theta\le 2\pi \tag{2}$$

$$=Re^{i\theta}\ , \tag{3}$$

where $R\equiv|\Phi|$.

To describe the gauge field, we refer to the work of Nielsen and Olesen [12] who obtain from their second equation of motion for flat space-time

$$A_\mu=\frac{1}{e^2}\frac{j_\mu}{|\Phi|^2}-\frac{1}{e}\partial_\mu\theta \tag{4}$$

$$=\frac{1}{e}[P-1]\phi_{,\mu}\ , \tag{5}$$

where $j_\mu\equiv\partial^\nu F_{\mu\nu}$, $P\theta_{,\mu}\equiv j_\mu/e|\Phi|^2$, and we have set $\theta=\phi$, the angular coordinate (see below). (We can now rewrite the equation for the scalar field as $\Phi=Re^{i\phi}$.) These expressions for A_μ and Φ will be used in our equations below and we will use R and P to characterize the scalar and gauge field, respectively. The Nielsen-Olesen vortex solution is a simple case of the U(1) strings which might appear in grand unified theories.

The equations of motion are given by

$$\frac{\partial L}{\partial\chi}=\nabla_\mu\frac{\partial L}{\partial(\partial_\mu\chi)}\ , \tag{6}$$

where χ is replaced by R, θ, or A_μ to give the three Euler-Lagrange equations. When A_μ is replaced by Eq. (5), the equation involving the derivatives with respect to θ is immediately satisfied, which is a consequence of our earlier choice of $\theta=\phi$. The covariant derivative ∇_μ requires the metric of the space-time to be specified.

We start by assuming that the space-time defined by the self-gravitating string has general cylindrical symmetry. The metric has the form

$$ds^2=-e^{2(K-U)}(dt^2-dr^2)+e^{-2U}W^2d\phi^2+e^{2U}dz^2\ , \tag{7}$$

where U, K, and W are unknown functions of r only and will be solved in our calculations.

Using this metric, the Euler-Langrange equations become

$$e^{2(U-K)}\left(R''+R'\frac{W'}{W}\right)-RP^2\frac{e^{2U}}{W^2}-\frac{dV}{dR}=0\ , \tag{8}$$

$$e^{2(U-K)}\left[P''-P'\left(\frac{W'}{W}-2U'\right)\right]-e^2R^2P=0\ , \tag{9}$$

where $\equiv\partial/\partial r$.

The energy-momentum tensor for the Lagrangian (1) is given by

$$T_{\mu\nu}=\frac{2}{\sqrt{-g}}\left\{\frac{\partial(\sqrt{-g}L)}{\partial g^{\mu\nu}}-\left(\frac{\partial(\sqrt{-g}L)}{\partial g^{\mu\nu}}\right)_{,\gamma}\right\}\ . \tag{10}$$

The components of T^μ_ν are

$$T^t_t=T^z_z=-\frac{e^{2(U-K)}}{2}\left[R'^2+\frac{e^{2K}}{W^2}R^2P^2+\frac{e^{2U}}{W^2e^2}P'^2+2Ve^{2K-2U}\right]\ , \tag{11}$$

$$T^r_r=\frac{e^{2(U-K)}}{2}\left[R'^2-\frac{e^{2K}}{W^2}R^2P^2+\frac{e^{2U}}{W^2e^2}P'^2-2Ve^{2K-2U}\right]\ , \tag{12}$$

$$T^\phi_\phi=\frac{e^{2(U-K)}}{2}\left[-R'^2+\frac{e^{2K}}{W^2}R^2P^2+\frac{e^{2U}}{W^2e^2}P'^2-2Ve^{2K-2U}\right]\ . \tag{13}$$

The Einstein equations $G^\mu_\nu=8\pi T^\mu_\nu$ that couple the string stress energy to its space-time geometry become

$$-2\frac{W''}{W}+2K'\frac{W'}{W}-2U'^2=8\pi\left[R'^2+\frac{e^{2K}}{W^2}R^2P^2+\frac{e^{2U}}{W^2e^2}P'^2+2Ve^{2K-2U}\right]\ , \tag{14}$$

$$2K'\frac{W'}{W}-2U'^2=8\pi\left[R'^2-\frac{e^{2K}}{W^2}R^2P^2+\frac{e^{2U}}{W^2e^2}P'^2-2Ve^{2K-2U}\right]\ , \tag{15}$$

$$2K''+2U'^2=8\pi\left[-R'^2+\frac{e^{2K}}{W^2}R^2P^2+\frac{e^{2U}}{W^2e^2}P'^2-2Ve^{2K-2U}\right]\ , \tag{16}$$

$$-2\frac{W''}{W}+4U'\frac{W'}{W}+4U''-2U'^2-2K''=8\pi\left[R'^2+\frac{e^{2K}}{W^2}R^2P^2+\frac{e^{2U}}{W^2e^2}P'^2+2Ve^{2K-2U}\right]\ . \tag{17}$$

These equations can be rearranged to give a simpler set of equations. The first simplification comes from Eq. (14) and (17), from which we obtain $K' = 2U' + \frac{C_1}{W}$. Since $W(0) = 0$ (see initial conditions), we set $C_1 = 0$ otherwise $K'(0) \to \infty$ and we run into numerical problems (assuming U' remains finite at the origin). Therefore, we directly obtain a relationship between K and U which is of the form $K = 2U + C_2$, where a new constant of integration is introduced. Since all solutions may be transformed such that $K(0) = U(0) = 0$, we set $C_2 = 0$ and therefore $K = 2U$.

By subtracting Eq. (14) from (15) we obtain an expression for W'':

$$W'' = -8\pi\left(\frac{e^{2K}R^2P^2}{W} + 2Ve^{2(K-U)}W\right) . \tag{18}$$

Using $K' = 2U'$, and (15) and (16) gives, for U'',

$$U'' = 4\pi\left(\frac{P'^2e^{2U}}{e^2W^2} - 2Ve^{2(K-U)}\right) - U'\frac{W'}{W} . \tag{19}$$

The field equations are integrable only if the conservation equations of energy and momentum $T^{\mu\nu}_{;\nu} = 0$ are satisfied. These conservation laws often give, analogous to the first integrals of classical mechanics, an important indication of how to solve the field equations. Using the energy-momentum tensor given above, the only nonvanishing component of the conservation equations is

$$R'\left[e^{2(U-K)}\left(R'' + R'\frac{W'}{W}\right) - RP^2\frac{e^{2U}}{W^2} - \frac{dV}{dR}\right] + P'\frac{e^{2U}}{e^2W^2}\left\{e^{2(U-K)}\left[P'' - P'\left(\frac{W'}{W} - 2U'\right)\right] - e^2R^2P\right\} = 0 . \tag{20}$$

Note that this equation is a linear combination of Eqs. (8) and (9) and therefore indicates that one of Eqs. (8) and (9) can be taken as redundant. Since the conservation of energy equation was derived from the Einstein equations, one of these equations can also be taken as redundant. We will take Eq. (15) as the redundant equation, which we will nevertheless continue using as a consistency check for our numerical integration, and keep both Eqs. (8) and (9). Equation (15) can be rewritten as

$$R'^2 = \frac{1}{4\pi}\left(K'\frac{W'}{W} - U'^2\right) + \frac{e^{2K}}{W^2}R^2P^2 - \frac{P'^2e^{2U}}{e^2W^2} + 2Ve^{2(K-U)} . \tag{21}$$

A complete set of equations consists of Eqs. (8), (9), (18), and (19), with Eq. (21) above. Similar results have been obtained by Garfinkle [13] and Laguna-Castillo and Matzner [9].

Putting $V = \alpha\frac{e^2}{8}(R^2 - \eta^2)^2$, $K = 2U$, $e^U = X$, and rescaling R by η, W and r by $\sqrt{8}/\eta e$ gives us the final set of equations to solve

$$X'' = \frac{1}{2}\pi\eta^2X^3\left(\frac{P'^2}{W^2} - 16\alpha(R^2-1)^2\right) + X'\left(\frac{X'}{X} - \frac{W'}{W}\right) , \tag{22}$$

$$W'' = -8\pi\eta^2X^2\left(X^2\frac{R^2P^2}{W} + 2\alpha W(R^2-1)^2\right) , \tag{23}$$

$$R'' = X^4\frac{RP^2}{W^2} + 4\alpha X^2R(R^2-1) - R'\frac{W'}{W} , \tag{24}$$

$$P'' = 8X^2R^2P + P'\left(\frac{W'}{W} - 2\frac{X'}{X}\right) , \tag{25}$$

$$R'^2 = \frac{1}{4\pi\eta^2}\frac{X'}{X}\left(2\frac{W'}{W} - \frac{X'}{X}\right) + X^2\left(X^2\frac{R^2P^2}{W^2} - \frac{P'^2}{8W^2} + 2\alpha(R^2-1)^2\right) . \tag{26}$$

Notice that the "e"'s all disappear from the equations. It can be interpreted as a scaling factor. We are left with a two-parameter set of equations instead of 3. The units that we chose to adopt in this paper are the natural units: $c = \hbar = G = 1$. In the original equations, R had units $[M]$, W and r, $[L]$, and P and X, $[1]$. After rescaling, the units of R, W and r have become [1] like the other variables. The dimensions of η, and e, λ and α are $[M]$ and [1], respectively. According to these units, the energy density will be expressed in terms of $[M]^4$.

III. INTEGRATION METHOD AND SOLUTIONS

For any given set of initial conditions, the differential equations determine the behavior of R, P, X, and W as a function of r. Although all solutions obtained from any initial set of conditions are valid solutions of the differential equations, we will examine in this work only solutions that exhibit the particular asymptotic behavior, for which $\lim_{r\to\infty} R = 1$ and $\lim_{r\to\infty} P = 0$. These conditions are derived from the requirement of finite action. Such solutions will be denoted as "unacceptable" solutions. They have the structure of a trapped vortex or string. Examples of an "acceptable" solution and some "unacceptable" solutions are portrayed in Fig. 1.

The two-point boundary-relaxation routine was used by LCM and by Garfinkle and Laguna to solve only for the scalar and gauge field differential equations using a specific background geometry. These authors then use a Runge-Kutta routine to solve the Einstein equations with the relaxation and initial value solution processes exchanging data. Thus theirs is a combination of relaxation and shooting methods. Our coupled differential equations *not only* describe the scalar and gauge field, for which there is a boundary condition at $r \to \infty$ but describe also the coupled gravitational field, for which

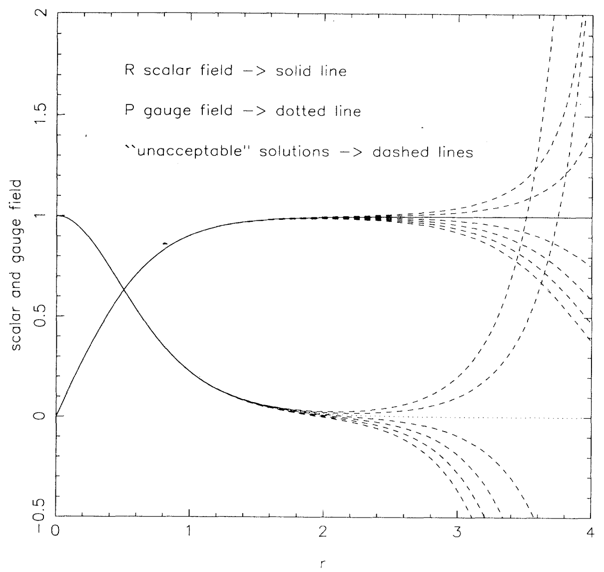

FIG. 1. The magnitude of the scalar and gauge field as a function of r and the difference between an "acceptable" and "unacceptable" solutions.

we cannot impose a boundary condition at large r unless an assumption is made about the spacetime structure there. We solved the coupled Euler-Lagrange-Einstein equations using a shooting method and searched the parameter space for all possible solutions.

A Taylor-series method was used to numerically integrate the set of five coupled differential equations. This method was chosen in part because of the flexibility of implementation at various orders, which allowed the same computer code to be used for both rapid exploration of parameter space followed by a more detailed study at a higher order of integration. In addition the use of a Taylor scheme, with the production of the higher order Taylor coefficients, allows direct calculation of many of the geometrical objects of interest (such as the Christoffel symbols or curvature tensors), without any need for data fitting or divided difference differentiations. Because of the complexity of the functions to be integrated, we used the REDUCE algebraic computing system to produce the mathematical expressions for the high order derivatives needed for the numerical integration. The transformation of the algebraic expressions to build the Taylor integration program in the C source code was done using the SCOPE package in REDUCE. The code so generated was verified to be correct by running the C source code back through REDUCE. This latter check is particularly important when using automated code production systems. Several consistency checks were applied to our solutions to ensure accuracy of the results. For example, the value of R' computed by the integration scheme was compared with that obtained from the redundant expression shown in Eq. (26).

The solutions of the differential equations are uniquely determined by a set of initial conditions. Recall that the variable U has been defined such that $U(0) = 0$ and therefore $X(0) = 1$. We also require that $R(0) = 0$, i.e., the axis is the region of false vacuum where the potential attains its local maximum. In order to define an axis, we must have $W(0) = 0$. Previous studies have required regularity on the axis and have imposed the condition that $\lim_{r\to\infty} g_{\phi\phi}/r^2 = 1$ (Garfinkle [13]). This means, in terms of our choice of coordinates, that $W'(0) = 1$. However, it is not clear that this condition is justified. For now, we will set $W'(0) = 1$ and will return to the case $W'(0) \neq 1$ in Sec. V. By asking that all derivatives be finite at the origin, we require that $P(0) = W'(0)$ and $X''(0) = \frac{\pi\eta^2}{4}\left(\frac{P''(0)^2}{W'(0)^2} - 16\alpha\right)$ while $W'(0), R'(0), P''(0)$ are undetermined and $X'(0), W(0), W''(0), R''(0), P'(0)$ vanish. An "acceptable" solution is therefore derived from those initial conditions, given the five free parameters $\eta, \alpha, W'(0), R'(0)$, and $P''(0)$.

The "acceptable" solutions form a particular subset of all solutions. The "goodness" of a solution is the deviation from the correct asymptotic structure and is measured by computing $\sqrt{R'^2 + P'^2}$ at large r. In agreement with Shaver, an "acceptable" solution is found at $\alpha = 1.0$, $\eta = 0.199\,471\,06$, $W'(0) = 1.0$, $R'(0) = 1.458\,608\,5$, and $P''(0) = -4.0$ with a deviation of $0.000\,036\,25$ measured at $r_{\max} = 4.0$ (our integration limit). From the precision on the parameters, one can see that to find an "acceptable" solution requires a very fine-tuning of the initial

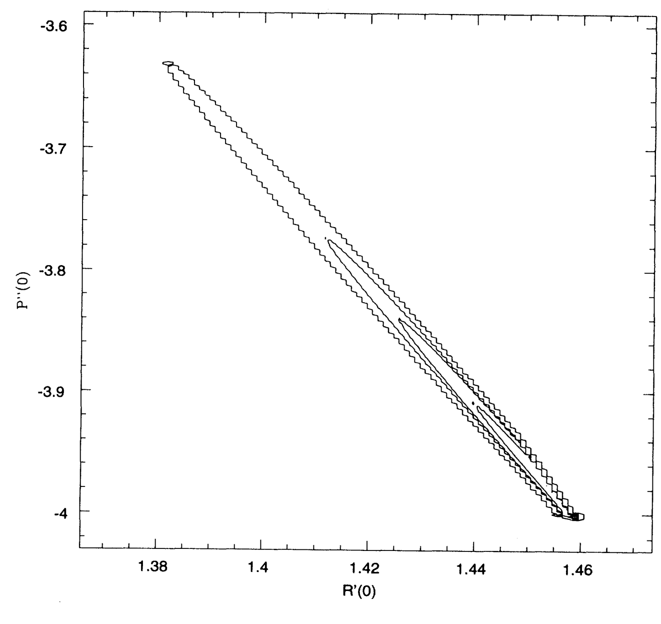

FIG. 2. Contour plot of the measured deviation from the correct asymptotic structure around the "acceptable" solution with parameters $\alpha = 1.0$, $\eta = 0.199\,471\,06$, $R'(0) = 1.458\,608\,5$, and $P'' = -4.0$. The contours are plotted for values of the deviation of 0, 0.5, 1, 2, 5, 10, 20, and 20 000. There is a deep valley very near the "acceptable" solution where the deviations get smaller than in the surrounding regions.

parameters. A small deviation in one of the input parameters causes a large deviation at $r_{\max}$ and gives an "unacceptable" solution. Finding "acceptable" solutions is therefore very difficult due to the strong coupling of the differential equations. Because of the "sharpness" of the valley of deviation of an "acceptable" solution (see Figs. 2 and 3), or, in other words, because of the precision required for the initial parameters, it is impossible to search randomly all parameter space in a reasonable time and hope to all on an "acceptable" solution. The approach we took for searching for "acceptable" solutions relies on the perturbation method of a known "acceptable" solution. By manually tuning the initial parameters for a perturbed solution and by using an extrapolation method to find the next "acceptable" solution, we were able to step away from the known solution and find the other "acceptable" solutions in the parameter space of all solutions. Our search through parameter space was a discrete search done for specific values of η with interpolation between found solutions. The subset obtained using this method covers the surfaces shown in Figs. 4 and 5. The ranges of the α and η parameters are such that α covers the region from 0.001 (α cannot be zero) to 2.5 and η, from 0.0 to 0.2.

A representative sample of solutions is shown in Figs. 6 and 7. The angular deficit is defined and discussed in Sec. V. If X and X' are set equal to 1, we recover Shaver's case. The first families of solutions, those with α constant, have $P''(0)$ and $X''(0)$ constant as well and show the same energy-momentum tensor. The special case of the Bogomol'nyi limit for which $\alpha = 1.0$ and $P''(0) = -4.0$ yield solutions which have no angular and radial energy-momentum components and have a metric of the form $X = 1.0$ and $W = br$, which represents the conical Minkowski spacetime where b is a constant and is directly related to the deficit angle by the relation $2\pi(1 - b)$ [see Fig. 6(a)]. This special case was studied in detail in Shaver [11] and Linet [16]. It was found that

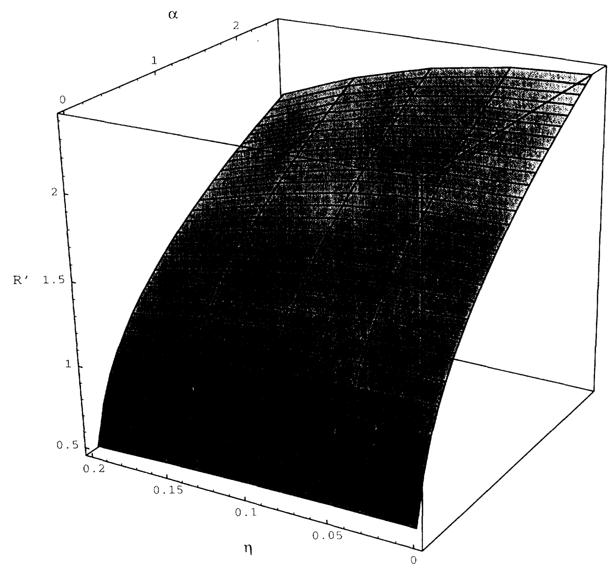

FIG. 4. Surface representing the subset of "acceptable" solution. The surface covers a range in α of 0.001 to 2.5 and a range in η of 0.0 to 0.2. This plot shows the value of $R'(0)$ for a specific choice of α and η parameters that will give an "acceptable" solution.

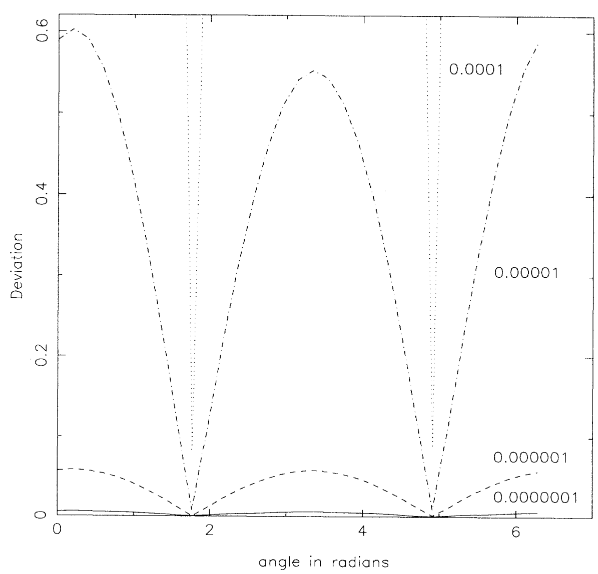

FIG. 3. Circular scans of the measured deviation shown in Fig. 2. Scans are drawn for circles of different radii around the "acceptable" solution. A complete circle is shown by an angle going from 0 to 2π as shown on the abscissa. The narrow valley of deviations is more apparent in this figure.

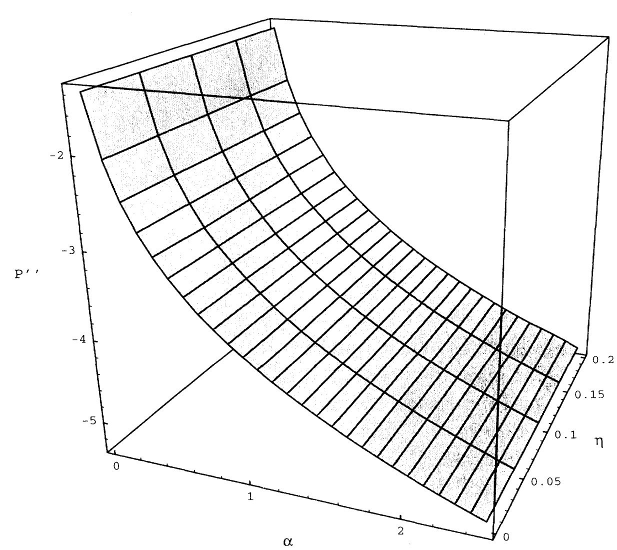

FIG. 5. For the same range as given in Fig. 4, this plot gives the value of $P''(0)$ for a specific choice of α and η parameters that will give an "acceptable" solution.

b depends on η and that keeping b positive requires that $\eta^2 < 4\pi$. The maximum value for η for these particular solutions is therefore ~ 0.2821. The angular deficits measured for this set of solutions are in agreement with Shaver and with LCM. The solutions with T^r_r and T^ϕ_ϕ non-null show a different linear energy density and deficit angle. This is due to the fact that the Gaussian curvature used to calculate the deficit angle, as described in Sec. V, depends on the energy-momentum tensor in the following way [15]:

$$K = 8\pi\left(T_{rr} + T_{\phi\phi} - \frac{1}{2}T\right) . \quad (27)$$

As we know, when the only nonvanishing component of the energy-momentum tensor is T^t_t, the angular deficit simply depends on the linear energy density of the string. For all computed energy-momentum tensor components, our values agree with Shaver and Garfinkle but disagree by a factor of 10 with the values obtained by LCM. It was also noted that LCM obtain a value of 3%, which is also what we obtain, for their value of $1-e^A$ (in our case, $1-X^2$) at $\eta = 0.01$ and $\alpha = 1/4$ (corresponding to our value of $\alpha = 4$) but quote a value of 0.03% in the text. It should be noted that a factor of 100 in this expression does make this solution meaningfully different from Minkowski spacetime. For the same families of solution, we also notice, in agreement with LCM, that the angular deficit and Weyl tensor are small for values of $\eta < 0.01$ and get larger and more important for $\eta > 0.01$ with increasing η. We also observe that the angular deficit and Weyl tensor increase with α. The Weyl tensor describes the shear in gravitational lensing and will be considered in Sec. VI.

IV. ASYMPTOTIC STRUCTURE

We know that the asymptotic behavior of the scalar and gauge field makes our solutions become either conical Minkowski spacetime or pure Minkowski spacetime as $r \to \infty$ (see Sec. V). We are interested in finding if the string can be finite in extent and have those conditions apply at a finite radius away from the origin thus providing a solution with an interior and ex-

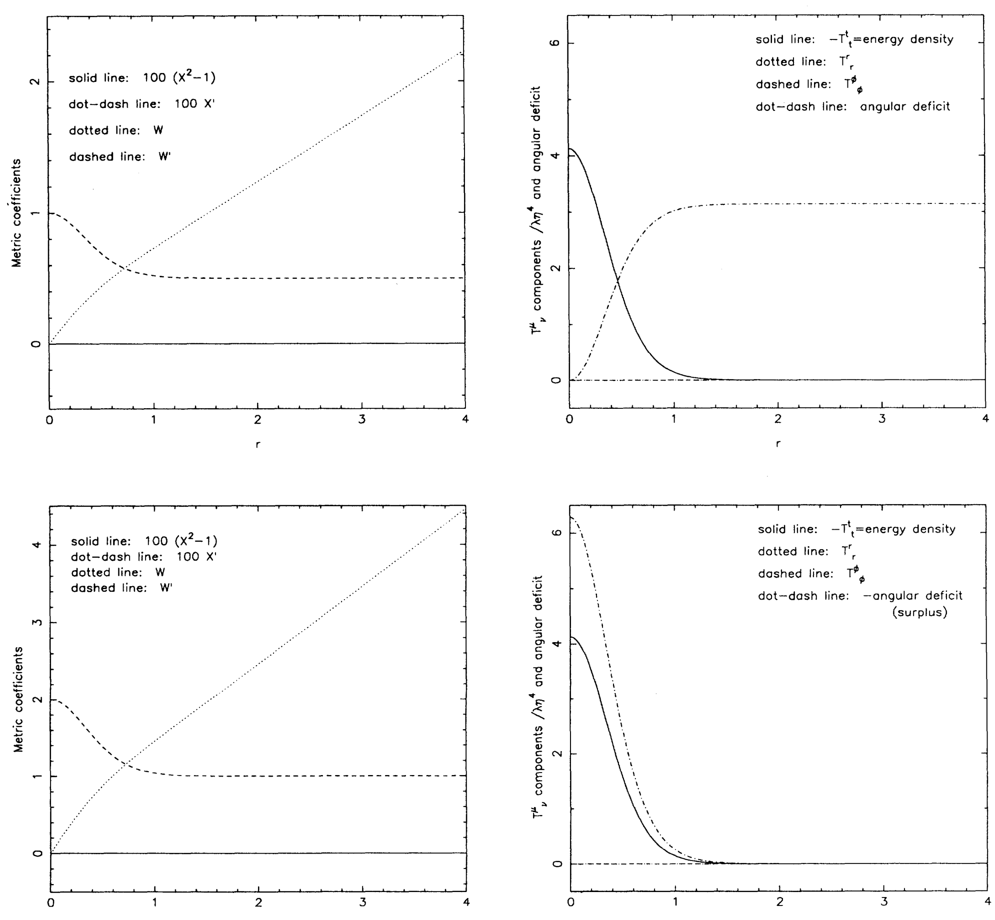

FIG. 6. Metric coefficients (left), energy-momentum tensor components, and angular deficit (right) of two representative string solutions of the Einstein-Euler-Lagrange equations. The top figures (a) corresponds to the solution with parameters $\alpha = 1.0$, $\eta = 0.199\,471\,06$, $W'(0) = 1.0$, $R'(0) = 1.458\,6085$, and $P''(0) = -4.0$ and the bottom figures (b) represent the solution with $\alpha = 1.0$, $\eta = 0.199\,471\,06$, $W'(0) = 2.0$, $R'(0) = 1.458\,6085$, and $P''(0) = -8.0$.

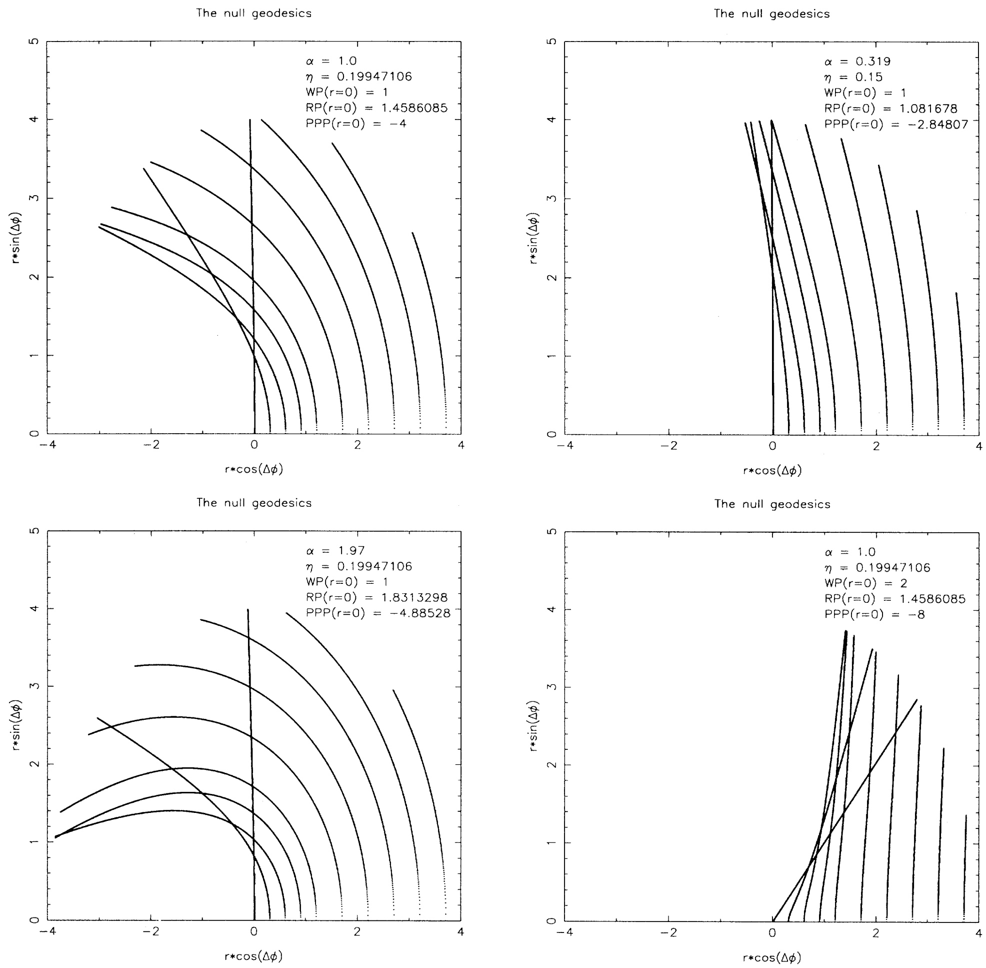

FIG. 7. Metric coefficients (left), energy-momentum tensor components, and angular deficit (right) of two more representative string solutions of the Einstein-Euler-Lagrange equations. The top figures (a) corresponds to the solution with parameters $\alpha = 0.319$, $\eta = 0.15$, $W'(0) = 1.0$, $R'(0) = 1.081\,678$, and $P''(0) = -2.848\,065$ and the bottom figures (b) represent the solution with $\alpha = 1.97$, $\eta = 0.199\,471\,06$, $W'(0) = 1.0$, $R'(0) = 1.831\,3298$, and $P''(0) = -4.885\,275$.

terior spacetime. Analytically, this can be easily verified by considering that at a finite radius r_0, the conditions $R''(r_0) = P''(r_0) = 0$ and $R'(r_0) = P'(r_0) = 0$ should apply. Keeping in mind that $W(0) = 0$ and $X(0) = 1$, it is straightforward to obtain from Eq. (25) that $P(r_0) = 0$ or $R(r_0) = 0$ and from Eq. (24) that $R(r_0) = 0$ or $R(r_0) = \pm 1$. From the asymptotic behavior of the gauge and scalar field we ask that $P(r_0) = 0$ and $R(r_0) = \pm 1$ be the values at $r = r_0$. From Eq. (23), we derive that $W''(r_0) = 0$ implying that $W'(r_0) = b$ and $W(r_0) = br$. From Eq. (26), $X'(r_0)/X(r_0) = 0$ with $X(r_0) = c$, or $2W'(r_0)/W(r_0) = X'(r_0)/X(r_0)$ with $X(r_0) = d(br^2)^2/2$, where c and d are constants. This last equation is not possible since $X(0)$ is not zero but 1. We therefore have $X(r_0) = c$. This analytic solution represents a conical Minkowski spacetime at $r = r_0$ or a pure Minkowski spacetime if $b = 1$.

We can see from these equations that requiring the spacetime to be conical Minkowski or pure Minkowski at a finite distance from the origin implies that the spacetime will be conical Minkowski or pure Minkowski everywhere, even at the origin. This confirms that the solutions we find only approach conical or pure Minkowski asymptotically: the string does not have a sharp, finite radius.

We defined a characteristic length λ for our string solutions by $\lambda = 1/(e\eta)$ [12] which measures the region over which the gauge field is appreciably different from zero (corresponding roughly to $r = 1$ in our radial coordinate system). If we assume that a grand unified theory (GUT) string has the same expression for λ and knowing that $\eta = 10^{15}$ GeV in that case, we can say that $r = 1$ corresponds approximately to 10^{-28} cm.

V. REGULARITY AT THE ORIGIN

The solutions we obtain when varying the parameter $W'(0)$ in addition to the other parameters mentioned above have the same $R'(0)$ (the same parameter space as shown in Fig. 4). The difference lies in the value of $P''(0)$, which is simply the value of $P''(0, W'(0) = 1)$ multiplied by $W'(0)$. The solution surface for $P''(0)$ is therefore the same as Fig. 5 scaled by $W'(0)$. This completes the solution space. We can compare solutions for which the only parameter varied is $W'(0)$. We find by setting $W'(0) = 2.0$ a new solution which has an asymptotic pure Minkowski spacetime instead of conical, currently associated with the solution $W'(0) = 1$ and other values of $W'(0) \neq 1$ as well.

In starting to look for solutions, we chose to set $W'(0) = 1$. This has been consistently assumed throughout the literature on cosmic strings, on the basis that $W'(0) = 1$ implies that the axis of the string is pure Minkowski, i.e., "free of conical singularities" [15]. There seem to be few arguments that lead to a justification of this particular assumption of regularity. We can write our metric in terms of the new coordinates as

$$ds^2 = -X^2(r)(dt^2 - dr^2) + \frac{W^2(r)}{X^2(r)}d\phi^2 + X^2(r)dz^2 \quad (28)$$

and impose the set of initial conditions derived in Sec. III, as $r \to 0$, $X \to 1$, and $W \to 0$, independently of the choice of W' at $r = 0$. There is then no singularity in the sense defined by the divergence of the Kretschmann scalar: $\mathcal{K} = \mathcal{R}^{\sigma\tau\mu\nu}\mathcal{R}_{\sigma\tau\mu\nu}$ where $R_{\sigma\tau\mu\nu}$ is the Riemann tensor. For the general metric given above, the Kretschmann scalar is given by

$$\begin{aligned}\mathcal{K} = \frac{4}{X^8W^2}(&3X''^2X^2W^2 - 10X''X'^2XW^2 \\ &+6X''X'W'X^2W - 2X''W''X^3W + 14X'^4W^2 \\ &-22X'^3W'XW + 6X'^2W''X^2W + 11X'^2W'^2X^2 \\ &-6X'W''W'X^3 + W''^2X^4)\end{aligned} \quad (29)$$

and does not diverge at the origin. The Gauss-Bonnet theorem can be used to calculate the angular deficit for a spacetime free of conical singularities, i.e., given a simply connected and regular surface bounded by a closed curve, the angle through which an arbitrary vector rotates when parallel transported around the curve is proportional to the integral of the curvature over the surface. For the metric given by Eq. (28), the integral of the Gaussian curvature K has the analytic form

$$\begin{aligned}\theta(R) &= 2\pi\int_0^R K(r)\sqrt{g}dr \\ &= 2\pi\frac{-1}{X(r)}\left(\frac{W'(r)X(r) - W(r)X'(r)}{X^2(r)}\right)\Bigg|_0^R \\ &= 2\pi[\xi(R) - \xi(0)]\ ,\end{aligned} \quad (30)$$

where $\xi(r)$ is the function given on the second line of Eq. (30) to be evaluated at R and 0 [17]. Because the spacetime is regular at the origin, $\xi(0) = -1$ and the angular deficit at R is $\theta(R) = 2\pi(\xi(R) + 1)$. The angular deficit becomes simply $2\pi(1 - b)$ if the spacetime is conical Minkowski at R. Returning to the Gauss-Bonnet theorem, we can also write

$$\begin{aligned}\theta(r2)\theta(r1) &= 2\pi\int_{r1}^{r2} K(r)\sqrt{g}dr \\ &= 2\pi\frac{-1}{X(r)}\left(\frac{W'(r)X(r) - W(r)X'(r)}{X^2(r)}\right)\Bigg|_{r1}^{r2} \\ &= 2\pi[\xi(r2) - \xi(r1)]\ .\end{aligned} \quad (31)$$

This equation does not require regularity at the origin and if $\lim_{r1\to 0}\theta(r1)$ is known, we can use it to find the angular deficit at $r2, \theta(r2)$. We can see that for a simple cone, Eq. (30) does not apply, but Eq. (31) gives the correct answer, namely that $\theta(r2) = \theta(r1)$ everywhere. Let us now evaluate the angular deficit outside the string, e.g., at $r = 4$, for two particular solutions mentioned above. The first one with $W'(0) = 1$ and $T^r_r = T^\phi_\phi = 0$, i.e., with regularity at the origin, has a value of $\xi(r = 4) = -0.5$ which represents a conical spacetime with angular deficit of $2\pi(-0.5 + 1) = \pi$ at $r = 4$. In this case, we could have simply used Eq. (30) to obtain the answer. The second particular solution with $W'(0) = 2$ and without regularity at the origin has a value of $\xi(r = 4) = -1, \xi(0) = -2$, and $\theta(0) = -2\pi$ in agreement with no deficit angle, i.e., $\theta(r = 4) = -2\pi + 2\pi(-1 + 2) = 0$ (see Fig. 6—note that for smaller values of $r, \theta(r)$ is negative and we refer to it as angular surplus). The spacetime is pure Minkowski at that distance from the origin. For the nonregular solutions, Eq. (30) does not apply but the angular deficit can still be computed using Eq. (31) which is an extension of the Gauss-Bonnet theorem.

VI. POSSIBILITY OF GRAVITATIONAL LENSING

The solutions we have derived introduce the possibility of the existence of cosmic strings in our universe which would produce gravitational lensing as long as the energy-momentum tensor is nonzero (it can be easily seen from the differential equations that if the energy-momentum tensor is zero, the spacetime is simply conical Minkowski or pure Minkowski and the lensing is geometrical). For our solutions, this occurs everywhere since the spacetime approaches conical Minkowski or pure Minkowski only asymptotically even though the stronger effects occur in a finite region around the origin. Assuming that the effective finite size of GUT strings is of the order of 10^{-28} cm, it seems unlikely that any gravitational lensing effects will be observable today from strings in our horizon volume. Nevertheless, the dynamics of strings (and GUT strings in particular) has not yet been worked out and it is possible that they may evolve in size so that their gravitational effects might be observed today. Also, realistic strings might form with a more complicated internal structure including condensates which would contribute to the T^r_r and T^ϕ_ϕ components of the energy-momentum tensor and therefore to the gravitational lensing effects. The limit imposed by Kaiser and Stebbins [14] on $G\mu$ for GUT strings cannot be considered rigid since their method for computing such a limit is not rigorous. In this section, we present the gravitational lensing effects and leave the discussion of the possibility of observing such effects to a later time.

The gravitational perturbation of cosmic strings on light rays produces real gravitational lensing which contrasts greatly with the geometrical lensing associated with the conical Minkowski spacetime. We first examine the null geodesics in the string spacetime describing our solutions.

The null geodesic equation for the string metric given by Eq. (28) can be expressed as

$$\frac{-E^2}{X^2(r)} + \frac{X^6(r)}{W^2(r)} L^2 \left(\frac{dr}{d\phi}\right)^2 + \frac{X^2(r)}{W^2(r)} L^2 = 0 \ . \qquad (32)$$

The geodesics are described in the plane $z =$ const. We can rewrite this equation in terms of functions of r_c, the closest approach radius where $dr/d\phi = 0$. This gives

$$\frac{d\phi}{dr} = \pm \frac{1}{\frac{W(r_c)}{X(r_c)} h\sqrt{h^2-1}} \ , \qquad (33)$$

where $h = \frac{W}{W(r_c)} / \left(\frac{X}{X(r_c)}\right)^2$. The $\pm$ sign in front of the expression on the right-hand side of the equation can be interpreted as the receding part of the orbit (+ sign) and the approaching part of the orbit (− sign).

Therefore, for the receding part of an orbit starting at r_c and finishing at large $r = r_{\rm max}$, the angle traversed can be computed using the integral:

$$\Delta\phi = \int_{r_c}^{r_{\rm max}} \frac{1}{\frac{W(r_c)}{X(r_c)} h\sqrt{h^2-1}} dr \ . \qquad (34)$$

For the case where $W(r)/X(r) = br$, this integral can be obtained analytically and, as expected, the angular deviation in the conical spacetime is constant:

$$\Delta\phi = \frac{1}{b} \cos^{-1}\left(\frac{r_c}{r}\right)\Bigg|_{r_c}^{r_{\rm max}} \ . \qquad (35)$$

This metric is conformally flat and one can apply a coordinate transformation and interpret the difference from pure Minkowski spacetime as the presence of a missing or surplus angle. For our solutions, there are no uniform conformal transformations which will make the metric pure Minkowski. The metric has real curvature and the string is a true gravitating string.

We use an eight-point Gauss-Legendre integration method to compute the orbit of a photon in the equatorial plane of the string. Care is required in the integration near the closest approach, due to the vanishing denominator, but this can be handled easily by using the limiting form near closest approach as given in Eq. (35). The orbits are plotted for representative string solutions and are shown for different closest approach radius in Fig. 8.

In discussing the null orbits, it is important to investi-

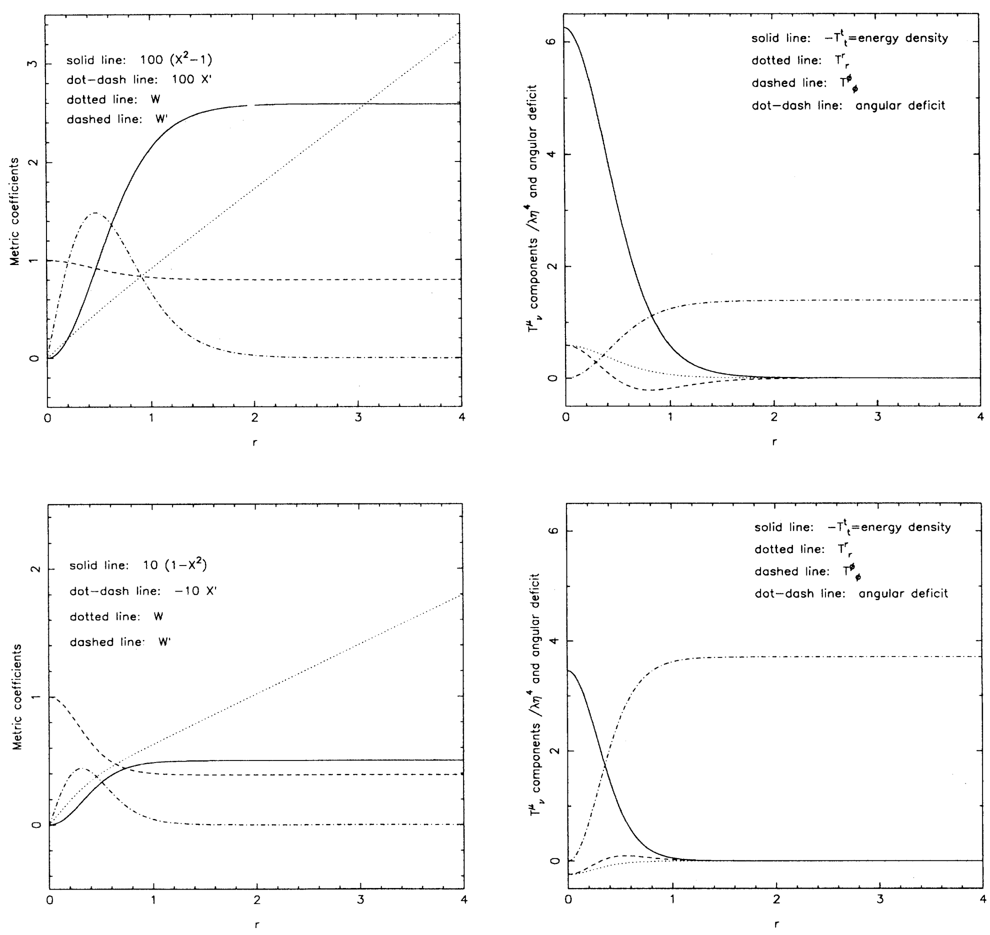

FIG. 8. The orbit of a photon in the equatorial plane of a cosmic string, plotted in terms of the cylindrical coordinates r and ϕ, for selected values of the closest approach radius of the orbit. The orbits depicted here are for the solution depicted in Figs. 6 and 7, with the upper left and upper right diagrams associated with Figs. 6(a) and 6(b), respectively, and with the lower left and lower right diagrams associated with Figs. 7(a) and 7(b).

gate the possible existence of an event horizon or a photon cylinder (in analogy to the photon sphere for the Schwarzschild spacetime) associated with our string solutions. To determine if the solutions we have found have a photon cylinder, we need to find the zeros of $dr/d\phi$. Examination of this function graphically shows that there is exactly one zero for each ray, that at closest approach, but no others. There can be no ray which spirals continuously into the string axis, and thus there is no photon cylinder. We also find that there is no event horizon by considering the possibility of nullity of the appropriate Killing vector.

We are interested as well in the Weyl tensor for different gravitating string solutions to determine whether or not there exist tidal effects since these can lead to an understanding of the distortion, shear, and rotation of the geodesics in the string spacetime. All nonvanishing components of the Weyl tensor can be obtained from the component

$$C_{trtr} = \frac{2X''XW - 6X'^2W + 4X'W'X - W''X^2}{6W} \quad (36)$$

by using the relations: $C_{rzrz} = -C_{trtr}, C_{tztz} = -2C_{trtr}$, $C_{t\phi t\phi} = \left(\frac{W}{X^2}\right)^2 C_{trtr}$, $C_{\phi z\phi z} = -C_{t\phi t\phi}$, and $C_{r\phi r\phi} = 2C_{t\phi t\phi}$. The fact that the Weyl tensor has nonzero components combined with the nonvanishing of the Ricci tensor leads to the conclusion that these string solutions will produce significant gravitational lens effects for null rays passing near the axis of the string. These effects are in strong contrast to the simple "prism" optical effect introduced by the traditional vacuum strings where both the Ricci and Weyl tensors are identically zero. Thus there will be real distortions and amplification of distant objects seen along lines of sight passing near these strings. Of course, in the static situation treated here, there can be no perturbations to the temperatures of distant sources, such as the cosmic background radiation.

VII. CONCLUSION

We have shown that the Einstein-Euler-Lagrange equations describing a gravitating cosmic string can be solved simultaneously and accurately using a Taylor series method. This method allows us to also study the physical properties of the string solutions for any set of initial parameters we wish to examine. We found that there exist strings solutions which have the angular surplus at the axis and are described by a spacetime asymptotically going to pure Minkowski spacetime. This contrasts greatly with the already known solution for strings which assumes regularity at the axis and which approaches conical Minkowski spacetime for large distance away from the axis of the string. The new solution is equally valid and the correct representation of the string spacetime might be one where the angular deficit (surplus) is localized and not known to the rest of the universe. Until we understand the dynamics of the string spacetime, we cannot say which is the correct representation of the string. We have shown that the string solutions given in this paper are characterized by significant gravitational lensing which might become important in the observation of strings once they have been described realistically using a dynamical model.

ACKNOWLEDGMENTS

We would like to thank Jody H. Palmer, Eric Shaver, and Glenn D. Starkman for many helpful discussions. This work has been supported by the Natural Sciences and Engineering Research Council of Canada through the Postgraduate program (F.R.M.) and an operating grant (C.C.D.).

[1] Q. Shafi and A. Vilenkin, Phys. Rev. D **29**, 1870 (1984).
[2] T. W. B. Kibble, G. Lazarides, and Q. Shafi, Phys. Lett. **113B**, 237 (1982).
[3] A. Vilenkin, Phys. Rev. D **23**, 852 (1981).
[4] Ya. B. Zel'dovich *et al.*, JETP **67**, 3 (1974).
[5] T. W. B. Kibble, J. Phys. A **9**, 1387 (1976).
[6] J. R. Gott, Astrophys. J. **288**, 422 (1985).
[7] W. A. Hiscock, Phys. Rev. D **31**, 3288 (1985).
[8] A. K. Raychaudhuri, Phys. Rev. D **41**, 3041 (1990).
[9] P. Laguna-Castillo and R. A. Matzner, Phys. Rev. D **36**, 3663 (1987).
[10] D. Garfinkle and P. Laguna, Phys. Rev. D **39**, 1552 (1989).
[11] E. Shaver, Gen. Relativ. Gravit. **24**, 187 (1992).
[12] H. B. Nielsen and P. Olesen, Nucl. Phys. **B61**, 45 (1973).
[13] D. Garfinkle, Phys. Rev. D **32**, 1323 (1985).
[14] N. Kaiser and A. Stebbins, Nature (London) **310**, 391 (1984).
[15] L. H. Ford and A. Vilenkin, J. Phys. A **14**, 2353 (1981).
[16] B. Linet, Class. Quantum Grav. **7**, L75 (1990).
[17] J. J. Stoker, in *Differential Geometry*, edited by R. Courant, L. Bers, and J. J. Stoker (Wiley-Interscience, New York, 1969).

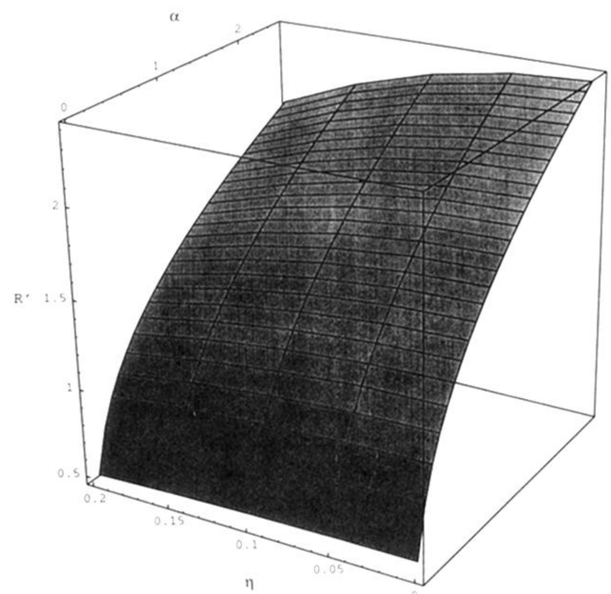

FIG. 4. Surface representing the subset of "acceptable" solution. The surface covers a range in α of 0.001 to 2.5 and a range in η of 0.0 to 0.2. This plot shows the value of $R'(0)$ for a specific choice of α and η parameters that will give an "acceptable" solution.

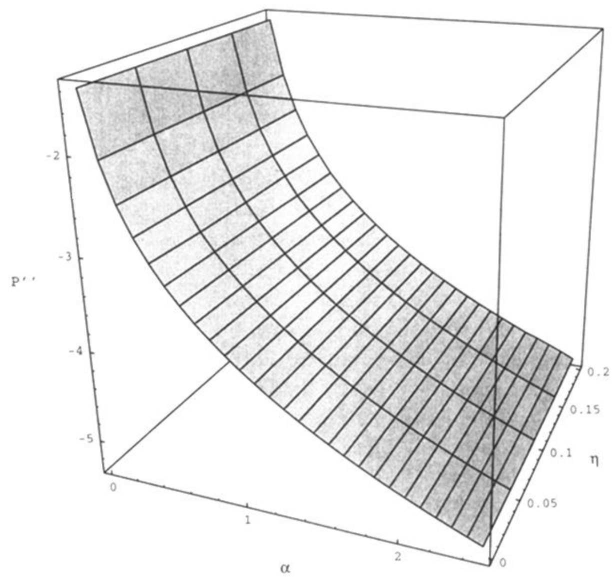

FIG. 5. For the same range as given in Fig. 4, this plot gives the value of $P''(0)$ for a specific choice of α and η parameters that will give an "acceptable" solution.